

## Estimation of Single Crop Coefficient and Crop Evapotranspiration Using Remote Sensing for Irrigation Management

Suhardi <sup>a,b,\*</sup>, Bambang Marhaenanto <sup>a</sup>, Joni Murti Mulyo Aji <sup>c</sup>

<sup>a</sup> Agricultural Engineering, Faculty of Agricultural Technology, University of Jember, Jember, 68121, East Java, Indonesia

<sup>b</sup> Doctoral Study Program of Agricultural Science, Faculty of Agriculture, University of Jember, Jember, 68121, East Java, Indonesia

<sup>c</sup> Department of Agribusiness, Faculty of Agriculture, University of Jember, Jember city, 68121, East Java, Indonesia

Corresponding author: \*hardi.ftp@unej.ac.id

**Abstract**— Indonesia has rainy and dry seasons sequentially from April to October and October to March. In the dry season, water availability in the soil gradually decreases, especially from June to October, when the peak of drought occurs, causing many agricultural lands to be left uncultivated. However, a small portion of agricultural land can still be planted for crops such as maize and groundnut. However, limited water availability causes crop growth to be disrupted because the amount of water absorbed by crop roots is less than the amount of evapotranspiration water. Therefore, an accurate evapotranspiration estimation technique is needed to make the water supply efficient. This study aims to evaluate the reliability of the technique of estimating crop coefficient (Kc) of maize and groundnut and temperature at the research location. A linear relationship between the Normalized Difference Vegetation Index (NDVI) from sentinel two imagery and Kc-FAO was used to estimate Kc. Meanwhile, a linear relationship between LST from Landsat 8 imagery and the results of interpolating temperature data from 4 climatological stations were used to estimate the temperature at the research site. The results of estimation showed that Kc of maize and groundnut were very accurate with the determinant coefficients ( $R^2$ ) respectively 0.8791 and 0.9352. This is similar to the results of the temperature estimation of the research location, showing a very accurate  $R^2$  is 0.9073. The results of this study are expected to be used for future research to improve water crop management.

**Keywords**— Sentinel 2; Landsat 8; crop coefficient; evapotranspiration; remote sensing.

Manuscript received 16 Jun. 2021; revised 12 Nov. 2022; accepted 3 Jan. 2023. Date of publication 30 Apr. 2023.  
IJASEIT is licensed under a Creative Commons Attribution-Share Alike 4.0 International License.



### I. INTRODUCTION

The dry season in Jember Regency, Indonesia, happens from June to October. Farmers crop corn and groundnuts in the dry season, considering that these two crops do not require much water (stagnant water). However, the calculation of water needs to be considered so that the water supply for crops is efficient. The limited availability of water in the soil will cause the growth of corn and groundnuts to be not optimal because of the inhibition of leaf stomata opening, which impacts crop metabolism and physiological processes. On the other hand, excessive water supply will decrease crop growth and production processes. Considering that water resources decrease during the dry season, it is necessary to calculate water so that the water supply for crops is more efficient.

The availability of water in the soil affects crop growth. Water functions as a constituent of the crop body, a solvent and a medium of biochemical reactions, a transport medium for compounds, a turgor for cells (indispensable for cell

division and enlargement), a raw material for photosynthesis, and keeps crop temperatures constant. The availability of water in the soil is very dependent on rainwater. Part of the rainwater that falls on the ground becomes runoff, partly seeps into the ground, and is stored in it. However, the water in the ground will become more limited when the dry season arrives, and the rate of evaporation and transpiration increases.

Evapotranspiration is a combination of evaporation and transpiration. Evaporation is the evaporation of water into the atmosphere through the soil surface, while transpiration is the process of evaporating water into the atmosphere through the stomata of living crops. Evapotranspiration in crops occurs due to climate change. This climate change is often identified based on the increase in temperature. Along with this increase in temperature, evapotranspiration also increases [1]. Evapotranspiration is also influenced by seasons, where for areas that experience flooding, the evaporation rate is higher when compared to areas with dry conditions [2]. On dry land, evapotranspiration is influenced by soil moisture, rainfall, and groundwater depth [3]. The duration of solar radiation, air

temperature, and wind speed also positively affect potential evapotranspiration, while relative humidity negatively affects potential evapotranspiration [4]. Meanwhile, the factors that affect evaporation are temperature differences, irradiation time, wind speed, and rainfall [5]

This evapotranspiration can be used to estimate crop water requirements. In the field of agricultural irrigation, evapotranspiration is divided into reference evapotranspiration (ET<sub>o</sub>) and crop evapotranspiration (ET<sub>c</sub>). ET<sub>o</sub> is atmospheric evaporation based on climatic parameters, while ET<sub>c</sub> refers to evapotranspiration from well-managed and well-watered land so that crops reach full production under certain climatic conditions [6]. ET<sub>o</sub> calculates crop evapotranspiration with single and multiple crop coefficients or the Shuttleworth-Wallace method [7].

The estimation of evapotranspiration can be done using empirical methods and the application of data analysis technology based on remote sensing. This remote sensing technology makes it easy to estimate parameters related to evapotranspiration [8]. Remote sensing can also be used to detect the status of water content in crops by calculating the visible and near-infrared (VIS/NIR) spectral index [9]. Several crop spectrum indices to estimate evapotranspiration include the Normalized Difference Vegetation Index (NDVI), Soil Adjusted Vegetation Index (SAVI), and Enhanced Vegetation Index (EVI). The spectrum index is often used to measure the absorption level of vegetation pigments (chlorophyll) in the red spectral area, and the level of reflection in the near-infrared spectral area is NDVI [10]. The NDVI principle relies on the fact that due to the spongy coating found on the backside, leaves reflect a lot of light in near-infrared, a stark contrast to most non-crop objects. When crops become dehydrated or stressed, the spongy layer floats, and the leaves reflect less NIR light but the same amount in the visible range. Thus, combining these two signals can mathematically help differentiate crops from non-crops and healthy crops from sick crops [11].

NDVI-based evapotranspiration estimation can be done by making a scatter plot as a triangle between the Land Surface Air Temperature (LST) and NDVI [12]. NDVI can also be used to estimate the value of crop coefficients (K<sub>c</sub>) through the NDVI and K<sub>c</sub> relationships from the ASCE 70 manual [13]. This study aims to evaluate the reliability of remote sensing-based crop coefficient estimation (K<sub>c</sub>) and Land Surface Temperature (LST) in calculating crop evapotranspiration (ET<sub>c</sub>) on maize and groundnuts using Sentinel 2 and Landsat 8 Oli imagery.

## II. MATERIAL AND METHODS

### A. Study Area

The research was conducted on agricultural land located in Arjasa District, Jember Regency, East Java, Indonesia, with average rainfall from April to October of 84.71 mm (low rainfall). This condition causes limited water resources for irrigation, so some agricultural lands are left empty, and some others are planted with maize, groundnut, and other secondary crops. However, limited water resources can interfere with crop growth if the existing water resources are not managed properly. Therefore, accurate estimation of evapotranspiration and crop coefficients (K<sub>c</sub>) will take a good

solution to manage agricultural water resources well and efficiently.

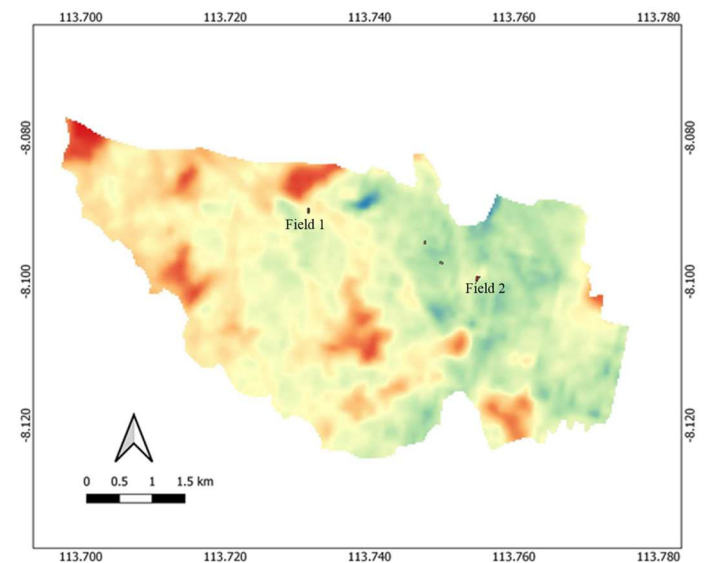


Fig. 1 Study area

### B. Datasets

This study uses satellite image datasets, including Sentinel 2 and Landsat 8 Oli (Table 1), as well as temperature data. The data period of sentinel 2 was June 2020 to November 2020. Sentinel 2 was used to calculate NDVI by utilizing band 8 (NIR) and band 4 (red), and it has been widely used by researchers [14], [15], [16], [17]. Sentinel 2A and Sentinel 2B were used in this study.

TABLE I  
SENTINEL 2 AND LANDSAT 8 IMAGERY DATA

No	Recording date	Satellite Name	Using
1.	Jun. 24, 2020. Jul. 4 and 24, 2020.	Sentinel 2B	NDVI analysis of maize crops
2.	Aug.8 and 18, 2020. Sept. 17, 2020. Oct 17. 2020	Sentinel 2A	NDVI analysis of maize crops and groundnut crops
3.	Jul. 24, 2020 Aug.23, 2020 Sept.12, 2020 Oct.2, 2020	Sentinel 2B	NDVI analysis of maize crops and groundnut crops
4.	Apr. 26, 2020 May 5 to 12, 2020 Aug. 9 to 25, 2020 Sept. 10, 2020.	Landsat 8	Calculation of LST

Table 1 above shows that the two sentinels are not much different except that the recording time at the same location has a difference of 5 days alternately [18]. Thus, the use of sentinels 2A and 2B together provides a greater opportunity

to observe the ground surface that is not covered by clouds [19]. Meanwhile, the Landsat 8 Oli and temperature data period is April 2020 to October 2020. The Data Landsat 8 Oli was used to calculate Land Surface Temperature (LST) [20]. The difference in data period of Sentinel 2 with Landsat 8 Oli and temperature was because the research location on Landsat 8 imagery is covered in clouds, so a longer data period is needed to obtain many Landsat 8 Oli image data minimum required to result in temperature predictions with very good accuracy. The temperature data used to calibrate the LST value was the average temperature on 4 Meteorology, Climatology, and Geophysics Agency (BMKG) stations in Banyuwangi, Sumenep, and Malang Regencies. The average temperature data were interpolated using the kriging method to produce the average temperature data at the study site.

### C. Single Crop Coefficient (Kc) Transformation Using the Normalized Difference Vegetation Index (NDVI)

Kc transformation using NDVI is carried out by looking for the relationship between the NDVI generated from the NDVI map and the single crop coefficient (Kc) value from the FAO table. NDVI can be used to estimate the value of Kc in the field at all crop phases [21]. Previous research also stated that the NDVI value has a trend that tends to be the same as the Kc [22]. Based on this description, the relationship between Kc and NDVI in this study uses the Generalized crop coefficient curve for the single crop coefficient approach (Figure 2) [6].

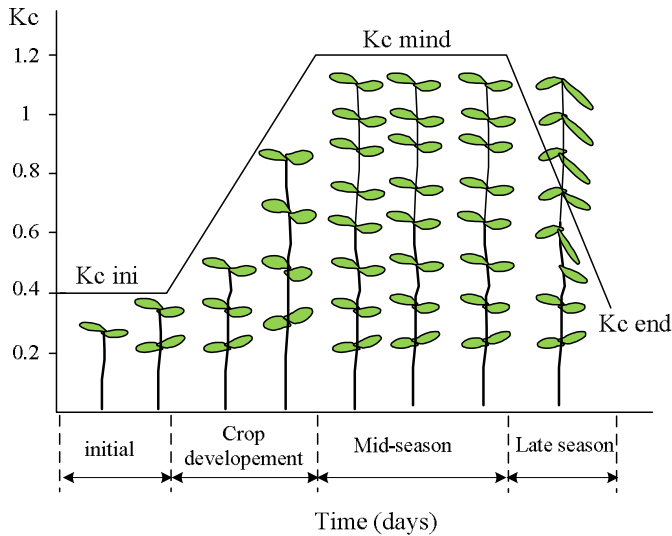


Fig. 2 The single crop coefficient approach from crop coefficient curve generalization

Linear regression was used to know the relationship between NDVI and Kc [13], [23]. Meanwhile, the NDVI calculation using the sentinel 2 image is written in equation 1 below.

$$NDVI = \frac{(R_{B8} - R_{B4})}{(R_{B8} + R_{B4})} \quad (1)$$

NIR and Red waves are selected in the NDVI calculation because leaf chlorophyll or pigment in leaves optimally absorbs light at a wavelength of 0.4 – 0.7  $\mu\text{m}$  during the photosynthesis process. Meanwhile, the leaf cell structure strongly reflects NIR light at a wave of 0.7 – 1.1  $\mu\text{m}$  [24].

### D. Transformation of Air Temperature Using Land Surface Air Temperature (LST)

Landsat 8 has two thermal infrared bands suitable for the Land Surface Air Temperature (LST) algorithm [25]. LST is important in hydrology, land cover, and global climate change. LST can be transformed using Landsat 8 band ten imagery. Metadata on the Landsat 8 band 10, namely thermal constant ( $K1 = 1321.08$  and  $K2 = 777.89$ ), rescaling factor ( $ML = 0.000342$  and  $AL = 0.1$ ), and correction value ( $O_i = 0.29$ ) are transformed into Brightness Air Temperature (BT) with equation 2 and 3 [26].

$$BT = \frac{K2}{\ln\left[\left(\frac{K1}{L\lambda}\right) + 1\right]} - 273.15 \quad (2)$$

$$T_s = \frac{BT}{\{1 + [\lambda BT / \rho] \ln \epsilon_\lambda\}} \quad (3)$$

$T_s$  is the LST in  $^{\circ}\text{C}$ ,  $\lambda$  is the wavelength of light (10,895). The Peak Value of the atmospheric spectral light ( $L\lambda$ ) generated from the Landsat 8 Band 10 was converted to the TOA Radiance spectral spectrum using the luminous resistance factor with the equation from the U.S. webpage Geological Survey (USGS).

$$L\lambda = M_L * Q_{cal} + A_L - O_i \quad (4)$$

$Q_{cal}$  is a calibrated and quantized standard product pixel value (DN). Meanwhile, emissivity ( $\epsilon_\lambda$ ) [27].

$$\epsilon_\lambda = \epsilon v P v + \epsilon s (1 - P v) + d \epsilon \quad (5)$$

$\epsilon v$  is the emissivity of the crop,  $\epsilon s$  is the emissivity of the soil,  $d \epsilon$  is the effect of reflection on the earth's surface ( $C = 0$  for flat surfaces) and  $C = 0.02$  for forests.

$$P v = \left( \frac{NDVI - NDVI_s}{NDVI_v - NDVI_s} \right)^2 \quad (6)$$

$P v$  is the proportion of NDVIv crops is 0.5, and  $NDVI_s$  is 0.2 for global conditions [28].

Previous research has shown a correlation between LST and air temperature [29]. Thus, the transformed LST from the Landsat 8 TIRS satellite image can be calibrated with air temperature to produce a calibration equation to calculate the LST data in the same period as the Kc data. Therefore, LST can be used to estimate the  $ET_o$  value [30].

### E. Estimation of Reference Evapotranspiration and Crop Evapotranspiration

Estimating reference evapotranspiration ( $ET_o$ ) using the Blaney-Criddle (BC) method. BC is very well used with very limited availability of climate data. The BC method was chosen because of its excellent performance in predicting evapotranspiration [31]. However, BC is not very accurate for predicting evapotranspiration with few parameters [32]. The Blaney-Criddle method can be written with equation 7 below.

$$ET_o = p(0,46T_{mean} + 8,13) \quad (7)$$

$ET_o$  is the reference evapotranspiration (mm / day), and  $p$  is the duration of exposure based on the FAO provisions. Meanwhile, crop evapotranspiration ( $ET_c$ ) is written by the following equation [6].

$$ET_c = Kc * ET_o \quad (8)$$

ETc is crop evapotranspiration (mm / day), Kc is cropping coefficient, and ETo is reference evapotranspiration (mm / day).

### III. RESULT AND DISCUSSION

#### A. Estimation of Kc for Maize and Groundnut

The crop coefficient (Kc) is a description of crop characteristics. The characteristics of a crop will change as the crop grows. Likewise, different types of crops have different characteristics. One of the crop characteristics used to detect Kc is leaf color. The greenness index value of this leaf can be calculated using the Normalized Difference Vegetation Index (NDVI) equation, which is the difference between reflected near-infrared (NIR) waves and red waves. The results of the calculations show that the NDVI value in maize tends to increase with the age of the crop, where the maximum NDVI value occurs at 63 days of age. NDVI values tend to decrease until the crops are ready to harvest (Figure 3). However, NDVI on groundnut crops showed a maximum value at the crop age of 91 days and was constant until harvest at 96 days. (Figure 4). The same thing was stated by Reyes-gonzález *et al.* [13] that the NDVI value in forage crops cropped in the spring was quite low until the third week after planting and

reached the maximum NDVI value at 11-12 weeks after planting.

Figure 5 shows that the NDVI Value curve and the single crop coefficient (Kc) curve listed in FAO 56 show relatively the same trend. The NDVI and Kc values for maize tended to increase and reached a maximum value at 63 days of planting, then NDVI and Kc decreased until the end of the planting season. Meanwhile, groundnut crop NDVI and Kc values increased and reached a maximum value at 96 days of the planting season. Based on this description, the value of Kc can be estimated using a graph of the relationship between the NDVI and Kc values from Table 12 FOA56. This method can be used as an alternative method of estimating the Kc value of crops at the research location (Figure 6).

Figure 6 shows that the correlation between NDVI and Kc of maize crops shows a very strong positive correlation with a value of  $R^2 = 0.8791$ , meaning that the NDVI value is very influential in estimating Kc of 87.91%. The correlation between NDVI and Kc of groundnut crops also shows a very strong positive correlation with a value  $R^2 = 0.9352$ , meaning that the NDVI value is very influential in estimating Kc of 93.52%. Thus, it can be argued that the NDVI value can be used to estimate the value of Kc in corn and groundnut crops grown in the Arjasa District, Jember Regency, East Java.

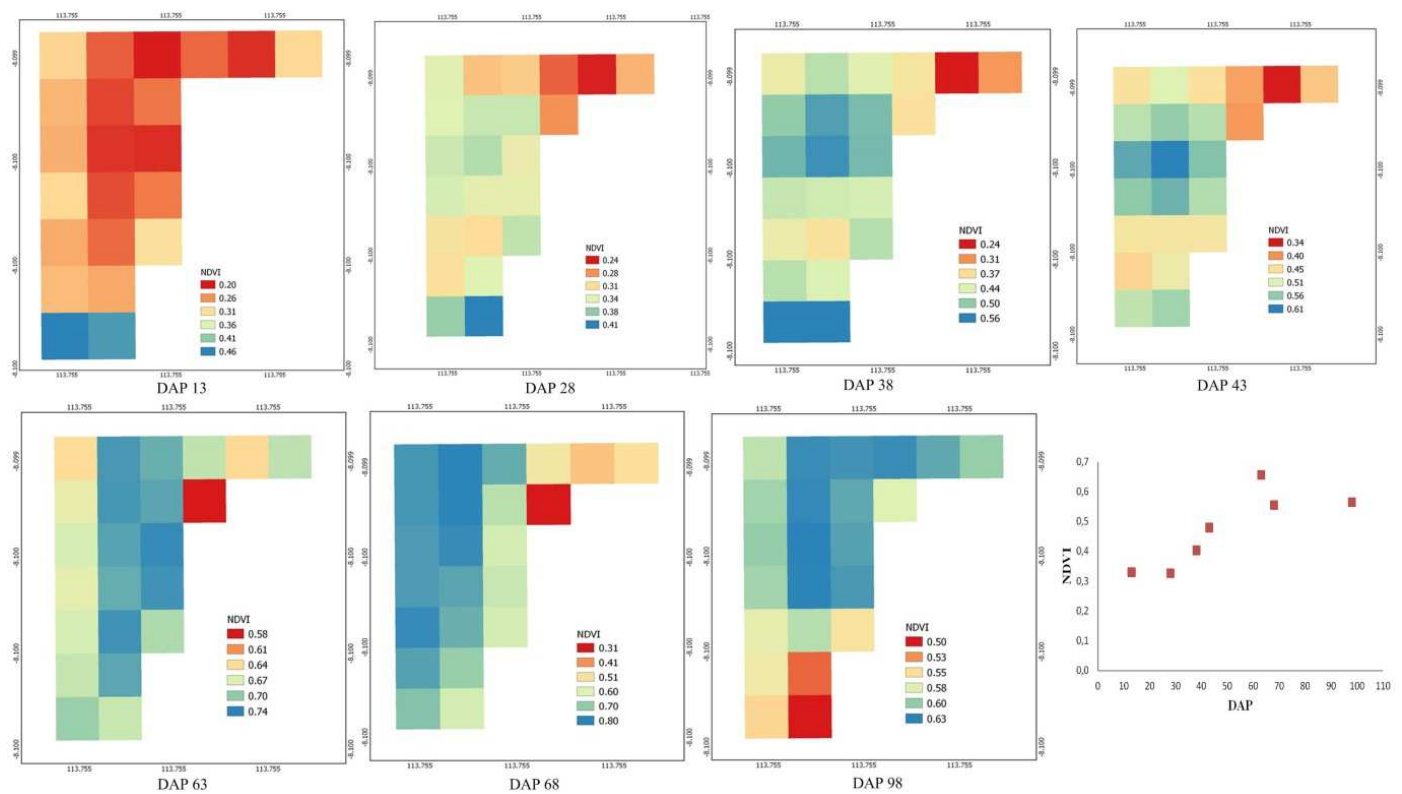


Fig. 3 Changes in NDVI value at cropping age of maize crops

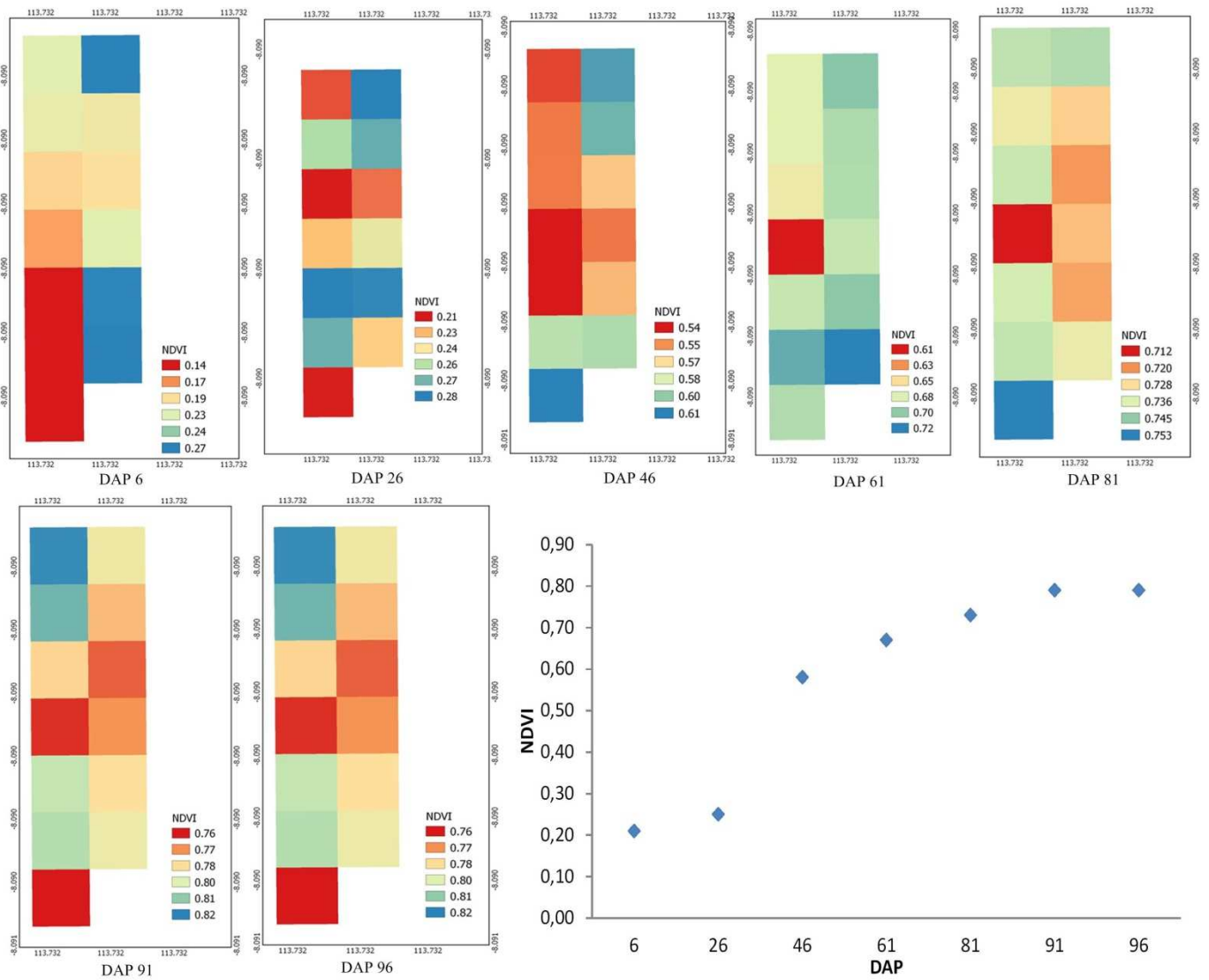


Fig. 4 Changes in NDVI values at cropping age of groundnut crops

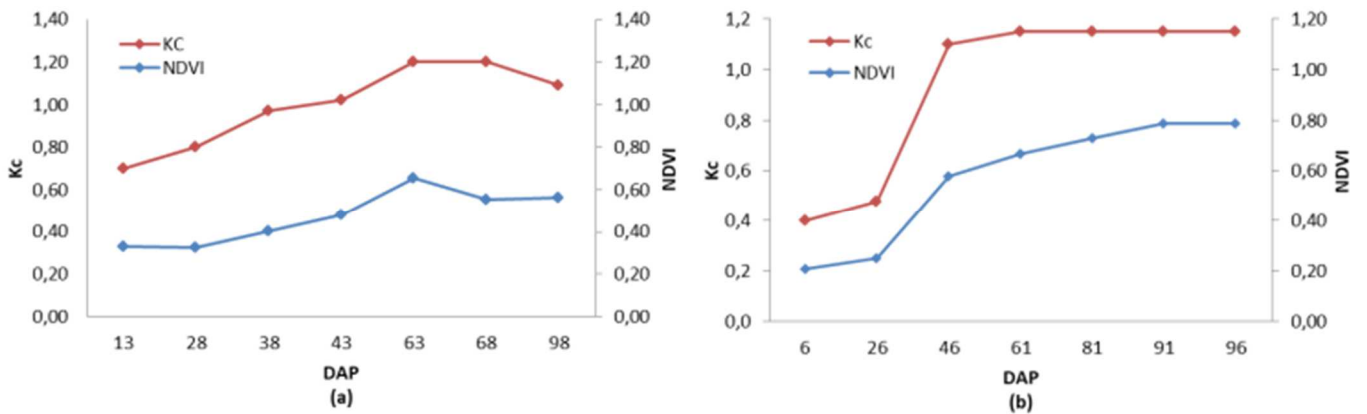


Fig. 5 The trend of NDVI value and single crop coefficient (Kc) in maize (a) and groundnut (b).

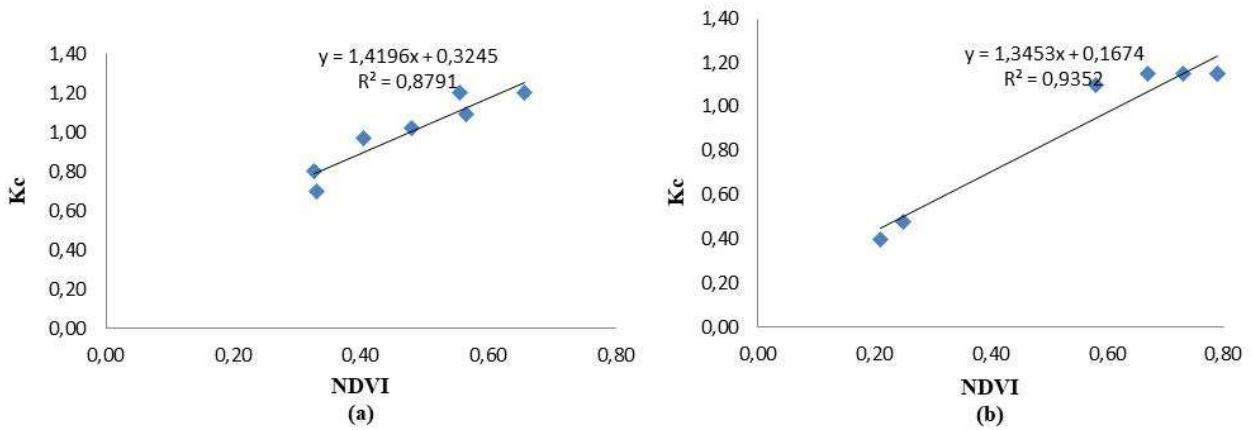


Fig. 6 The linear relationship between NDVI and Kc for maize (a) and groundnut (b)

### B. Transformation and Land Surface Calibration Air Temperature

The transformation of the value of Land Surface Air Temperature (LST) with units of degrees Celsius (°C) based on remote sensing uses Landsat 8 band ten satellite imagery. The LST transformation uses Open-Source Quantum GIS (QGIS) Software. The recording period of Landsat 8 imagery used was six periods of data recording, as shown in Figure 7. The selection of 6 image data for the recording period was based on the consideration that the selected image indicated that the research location was free from clouds. Cloud cover at the research location will affect the accuracy of the LST transformation results. In cloudy conditions, the LST value does not describe the air temperature conditions of the study location. Based on the results of the LST transformation on cloudy images, the LST value is low; this indicates that the result of the analysis of the resulting LST value comes from clouds. This is similar to the income stated by Akinyemi, Ikanyeng, and Muro [33] that the decrease in LST analysis results in images with cloud cover may occur due to the

inclusion of cloud temperature in the surface temperature analysis.

The LST transformation image is cropped according to the research location, so it is easier to present the air temperature of the research location. To determine the accuracy of the LST transformation results, it is necessary to calibrate with air temperature data measured by the Meteorology, Climatology, and Geophysics Agency (BMKG), the official government agency for managing and surveying climate data. Air temperature data were taken at 4 BMKG station locations in the East Java region, the closest station to the research location.

The four BMKG stations include the Banyuwangi Meteorological Station located in Banyuwangi Regency, Malang Climatology Station located in Malang Regency, Pasuruan Geophysical Station located in Pasuruan Regency, and Kalianget Meteorological Station located in Sumenep Regency, Madura Island. Therefore, the air temperature data from the four stations were interpolated using the kriging method to produce combat data at the research location, as shown in Figure 8.

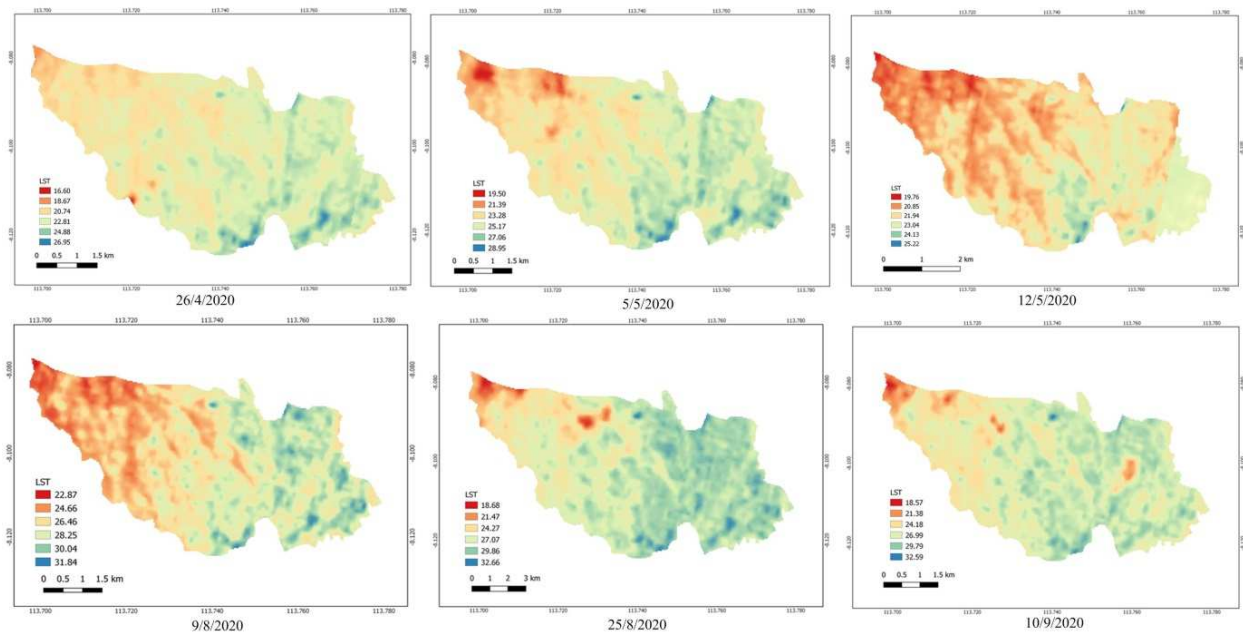


Fig. 7 LST transformed using Landsat 8 satellite imagery

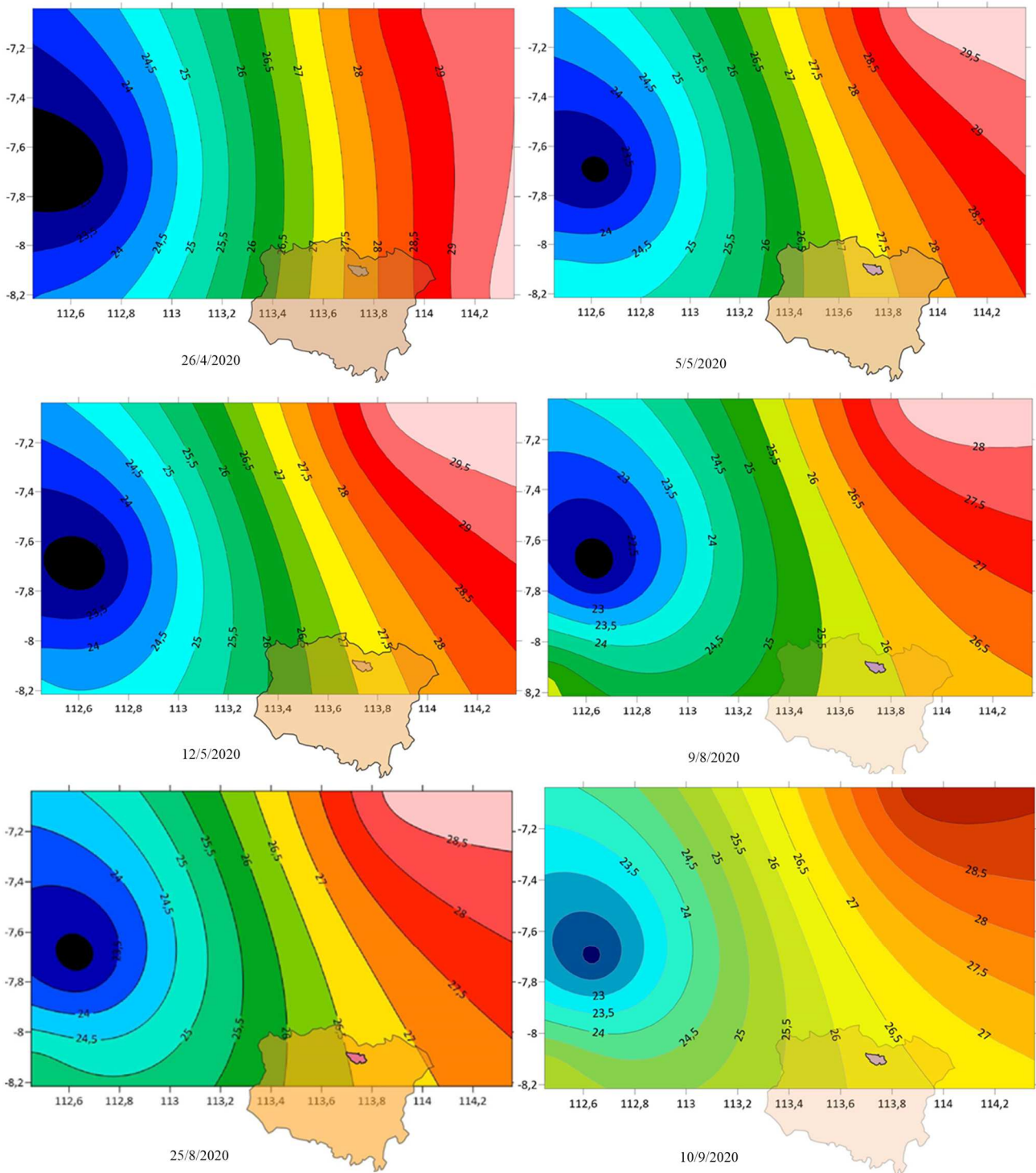


Fig. 8 Interpolation of air temperature data from 4 BMKG stations

Figure 8 shows that the resulting average air temperature is the average air temperature of the four BMKG stations with the same period as the Landsat 8 satellite image recording. It aims to calibrate the transfused LST data with air temperature data from the interpolated BMKG data. The research location, namely the Arjasa District area of Jember Regency, is displayed on the air temperature map so that the interpolation value at the research location can be determined easily. Furthermore, the air temperature data from the interpolation results were calibrated with LST data from remote sensing

using linear equations, as shown in Figure 9. The relationship between the average LST and the average air temperature at the study site shows a very strong negative correlation where the determinant efficiency value ( $R^2$ ) was 0.9073. This shows that if the air temperature rises  $1^\circ\text{C}$ , it will reduce LST by  $2.445^\circ\text{C}$ . Thus, it can also be argued that this average LST value can be used as average air temperature data to calculate reference evapotranspiration (ET<sub>o</sub>) with the FAO 56 Blaney-Criddle equation.

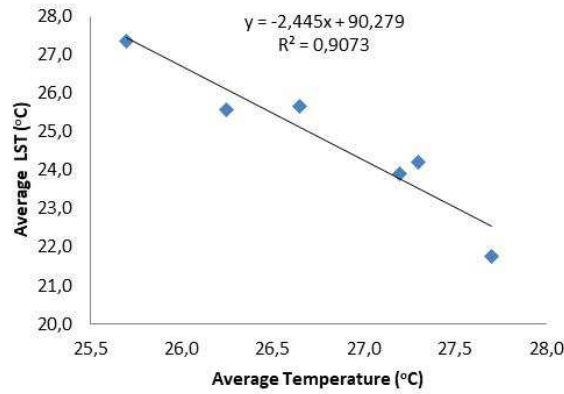


Fig. 9 The relation between average LST (°C) and average temperature (°C)

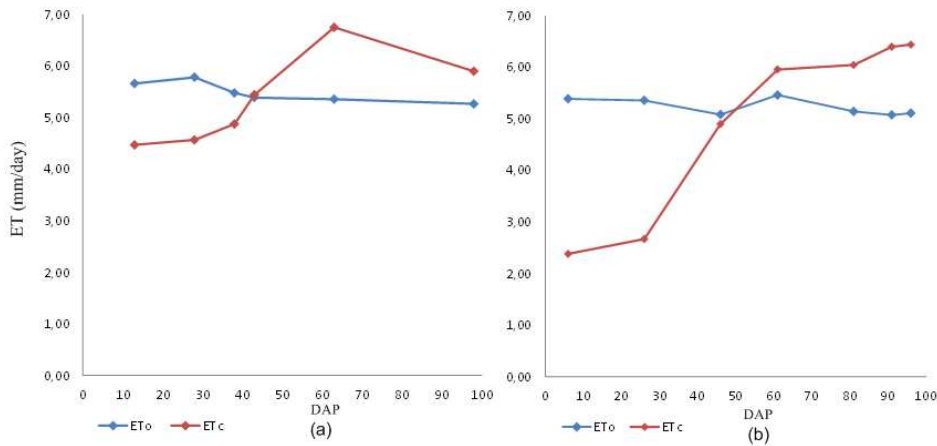


Fig. 10 Reference evapotranspiration (ETo) and crop evapotranspiration (ETc) in maize (a) and groundnut (b)

### C. Calculation of Crop Evapotranspiration (ETc)

The difference in the recording date of Sentinel 2 and Landsat 8 images is very influential in calculating remote sensing-based ETo. Therefore, the average temperature (Tmean) data at the study location from BMKG was converted into LST using the equation  $LST = -2.445 T_{mean} + 90.279$ . Thus, the LST data period can be adjusted to the period of Kc data resulting from the NDVI conversion using the equation  $Kc_{Groundnut} = 1.4764NDVI + 0.3144$  dan  $Kc_{maize} = 1.4196NDVI + 0.3245$ . Next, an estimation of reference evapotranspiration (ETo) is carried out using equation 7 on crops maize (DAP 13, 28, 38, 43, 63, and 98) and groundnuts (DAP 6, 26, 46, 61, 81, and 91). Meanwhile, the calculation of crop evapotranspiration uses equation 8. The results of ETo and ETc calculations can be seen in Figures 10 and 11 below.

Figure 10 shows that the ETo-Blaney-Criddle on land cropped with maize (a) and groundnut (b) tends to decrease from the beginning of the season to the harvest time; this is because the average LST has a climate parameter that has negative isolation to the average air temperature. Meanwhile, ETc in maize showed an increase during the growing period (DAP 28 - 63), ranging from 4.57 to 6.75 mm/day, and subsequently decreased until the harvest period (DAP 98) of 5.90 mm/day. However, the ETc in groundnuts tended to increase from the growing period to the near-harvest period (DAP 26 - 96), ranging from 2.67 to 6.44 mm/day. This shows that the canopy cover during the growing period of corn and

groundnuts affects the increase in ETc. This is similar to the opinion [13] that ETc is low in the early stages of vegetation and is higher until nearing harvest time, so the irrigation scheduling for dry and semi-arid areas must pay attention to the ETc value.

### IV. CONCLUSION

The method of estimating crop coefficient (Kc) on maize and groundnut crops based on remote sensing using Sentinel 2 imagery is done by making a linear relationship between the NDVI value and the Generalized crop coefficient curve for the single crop coefficient approach. The estimation results show very accurate results where the correlation between NDVI and Kc of maize and groundnut crops shows a very strong positive correlation with R<sup>2</sup> values of 0.8791 and R<sup>2</sup> of 0.9352. Meanwhile, the estimated average temperature at the study location using Landsat 8 imagery shows an extraordinarily strong negative correlation between the average temperature value and the Land Surface Temperature (LST) with R<sup>2</sup> is 0.9073. Thus, the NDVI value can be used to estimate the Kc of maize and groundnut crops. At the same time, the LST value can be used to estimate the average temperature. Thus, the Kc value from the NDVI transformation results and the temperature value from the LST transformation results can be used to calculate the ETc value. The results of this study are expected to be used for future research to improve the efficiency of crop water management.

## ACKNOWLEDGMENT

The authors thank the farmers permitted to research their agricultural land and all who have contributed to this research.

## REFERENCES

- [1] Q. Zhang, Z. Yang, X. Hao, and P. Yue, "Conversion features of evapotranspiration responding to climate warming in transitional climate regions in northern China," *Clim. Dyn.*, vol. 52, no. 7–8, pp. 3891–3903, 2019, doi: 10.1007/s00382-018-4364-3.
- [2] E. Eichelmann *et al.*, "The effect of land cover type and structure on evapotranspiration from agricultural and wetland sites in the Sacramento–San Joaquin River Delta, California," *Agric. For. Meteorol.*, 2018, doi: 10.1016/j.agrformet.2018.03.007.
- [3] X. Sun, B. P. Wilcox, and C. B. Zou, "Evapotranspiration partitioning in dryland ecosystems: A global meta-analysis of in situ studies," *J. Hydrol.*, vol. 576, no. June, pp. 123–136, 2019, doi: 10.1016/j.jhydrol.2019.06.022.
- [4] W. Dong, C. Li, Q. Hu, F. Pan, J. Bhandari, and Z. Sun, "Potential Evapotranspiration Reduction and Its Influence on Crop Yield in the North China Plain in 1961–2014," *Hindawi Adv. Meteorol.*, vol. 2020, p. 10, 2020, doi: 10.1155/2020/3691421.
- [5] Dwipa, I., Kasim, M., Rozen, N., & Nurhamidah, N. (2020). Land flooding effect Before and After Planting on Rice Yield in System Of Rice Intensification. *International Journal on Advance Science Engineering Information Technology*, 10(3).
- [6] R. G. Allen, L. S. Pereira, D. Raes, and M. Smith, *FAO Irrigation and Drainage Paper No. 56*, vol. 13, no. 3. Roma: FAO - Food and Agriculture Organization of the United Nations, 1998.
- [7] K. Xiang, Y. Li, R. Horton, and H. Feng, "Similarity and difference of potential evapotranspiration and reference crop evapotranspiration – a review," *Agric. Water Manag.*, vol. 232, no. January, 2020, doi: 10.1016/j.agwat.2020.106043.
- [8] R. Filgueiras *et al.*, "Soil water content and actual evapotranspiration predictions using regression algorithms and remote sensing data," *Agric. Water Manag.*, vol. 241, no. June, p. 106346, 2020, doi: 10.1016/j.agwat.2020.106346.
- [9] A. Ribera-Fonseca, E. Jorquera-Fontena, M. Castro, P. Acevedo, J. C. Parra, and M. Reyes-Díaz, "Exploring VIS/NIR reflectance indices for the estimation of water status in highbush blueberry plants grown under full and deficit irrigation," *Sci. Hortic. (Amsterdam)*, vol. 256, no. June, p. 108557, 2019, doi: 10.1016/j.scienta.2019.108557.
- [10] N. Mzid, V. Cantore, G. De Mastro, R. Albrizio, M. H. Sellami, and M. Todorovic, "The Application of Ground-Based and Satellite Remote Sensing for Estimation of Bio-Physiological Parameters of Wheat Grown Under Different Water Regimes," *Water*, vol. 12, no. 8, p. 2095, 2020, doi: 10.3390/w12082095.
- [11] U. Mahajan and B. R. Bundel, "Drones for Normalized Difference Vegetation Index (NDVI), to Estimate Crop Health for Precision Agriculture: A Cheaper Alternative for Spatial Satellite Sensors," in *International Conference on Innovative Research in Agriculture, Food Science, Forestry, Horticulture, Aquaculture, Animal Sciences, Biodiversity, Ecological Sciences and Climate Change (AFHABEC-2016)*, 2016, no. January, pp. 38–41.
- [12] J. M. Chen and J. Liu, "Evolution of evapotranspiration models using thermal and shortwave remote sensing data," *Remote Sens. Environ.*, vol. 237, no. December 2019, p. 111594, 2020, doi: 10.1016/j.rse.2019.111594.
- [13] A. Reyes-gonzález *et al.*, "Estimation of Crop Evapotranspiration Using Satellite Remote Sensing-Based Vegetation Index," *Adv. Meteorol.*, vol. 2018, no. 1, 2018.
- [14] C. J. Harmse, H. Gerber, and A. Van Niekerk, "Evaluating Several Vegetation Indices Derived from Sentinel-2 Imagery for Quantifying Localized Overgrazing in a Semi-Arid Region of South Africa," *Remote Sens.*, vol. 14, no. 1720, p. 18, 2022, doi: 10.3390/rs14071720.
- [15] H. K. Zhang *et al.*, "Characterization of Sentinel-2A and Landsat-8 top of atmosphere, surface, and nadir BRDF adjusted reflectance and NDVI differences," *Remote Sens. Environ.*, vol. 215, no. April, pp. 482–494, 2018, doi: 10.1016/j.rse.2018.04.031.
- [16] S. R. Karlsen, L. Stendardi, H. Tømmervik, L. Nilsen, I. Arntzen, and E. J. Cooper, "Time-series of cloud-free sentinel-2 ndvi data used in mapping the onset of growth of central spitsbergen, svalbard," *Remote Sens.*, vol. 13, no. 15, pp. 1–14, 2021, doi: 10.3390/rs13153031.
- [17] K. Yang, Y. Luo, M. Li, S. Zhong, Q. Liu, and Xiuhong Li, "Reconstruction of Sentinel-2 Image Time Series Using Google Earth Engine," *Remote Sens.*, vol. 14, no. 4395, p. 24, 2022.
- [18] E. Firmansyah, J. Gaol, and etyo B. Susilo, "Comparison of SVM and Decision Tree Classifier with Object Based Approach for Mangrove Mapping to Sentinel-2B Data on Gili Sulat, Lombok Timur," *J. Nat. Resour.*, vol. 9, no. 3, pp. 746–757, 2019, doi: 10.29244/JPSL.9.3.746-757.
- [19] J. Li and D. P. Roy, "A global analysis of Sentinel-2a, Sentinel-2b and Landsat-8 data revisit intervals and implications for terrestrial monitoring," *Remote Sens.*, vol. 9, no. 902, pp. 1–17, 2017, doi: 10.3390/rs9090902.
- [20] S. Li, J. Wang, D. Li, Z. Ran, and B. Yang, "Evaluation of landsat 8-like land surface temperature by fusing landsat 8 and modis land surface temperature product," *Processes*, vol. 9, no. 12, pp. 1–19, 2021, doi: 10.3390/pr9122262.
- [21] Y. Zhang, W. Han, X. Niu, and G. Li, "Maize crop coefficient estimated from UAV-measured multispectral vegetation indices," *Sensors (Switzerland)*, vol. 19, no. 23, pp. 1–17, 2019, doi: 10.3390/s19235250.
- [22] S. K. Dingre, S. D. Gorantiwar, and S. A. Kadam, "Correlating the field water balance derived crop coefficient (Kc) and canopy reflectance-based NDVI for irrigated sugarcane," *Precis. Agric.*, vol. 22, no. 4, pp. 1134–1153, 2021, doi: 10.1007/s11119-020-09774-8.
- [23] H. Niu, D. Wang, and Y. Chen, "Estimating Crop Coefficients Using Linear and Deep Stochastic Configuration Networks Models and UAV-Based Normalized Difference Vegetation Index Estimating Crop Coefficients Using Linear and Deep Stochastic Configuration Networks Models and UAV-Based Norm," 2020, no. September, pp. 1485–1490, doi: 10.1109/ICUAS48674.2020.9213888.
- [24] R. Wikantiyoso, A. G. Sulaksono, and T. Suhartono, "Detection of potential green open space area using landsat 8 satellite imagery," *ARTEKS J. Tek. Arsit.*, vol. 6, no. 1, pp. 149–154, 2021, doi: 10.30822/arteks.v6i1.730.
- [25] L. Wang, Y. Lu, and Y. Yao, "Comparison of three algorithms for the retrieval of land surface temperature from landsat 8 images," *Sensors (Switzerland)*, vol. 19, no. 22, 2019, doi: 10.3390/s19225049.
- [26] U. Avdan and G. Jovanovska, "Algorithm for automated mapping of land surface temperature using LANDSAT 8 satellite data," *J. Sensors*, vol. 2016, 2016, doi: 10.1155/2016/1480307.
- [27] J. A. Sobrino, J. C. Jiménez-Muñoz, and L. Paolini, "Land surface temperature retrieval from LANDSAT TM 5," *Remote Sens. Environ.*, vol. 90, no. 4, pp. 434–440, 2004, doi: 10.1016/j.rse.2004.02.003.
- [28] F. Wang, Z. Qin, C. Song, L. Tu, A. Karnieli, and S. Zhao, "An improved mono-window algorithm for land surface temperature retrieval from landsat 8 thermal infrared sensor data," *Remote Sens.*, vol. 7, no. 4, pp. 4268–4289, 2015, doi: 10.3390/rs70404268.
- [29] J. Cao, W. Zhou, Z. Zheng, T. Ren, and W. Wang, "Within-city spatial and temporal heterogeneity of air temperature and its relationship with land surface temperature," *Landsc. Urban Plan.*, vol. 206, no. November 2020, p. 103979, 2021, doi: 10.1016/j.landurbplan.2020.103979.
- [30] M. A. El-Shirbeny, B. Abdellatif, A. E. M. Ali, and N. H. Saleh, "Evaluation of Hargreaves based on remote sensing method to estimate potential crop evapotranspiration," *Int. J. GEOMATE*, vol. 11, no. 1, pp. 2143–2149, 2016, doi: 10.21660/2016.23.1122.
- [31] H. R. Fooladmand and S. H. Ahmadi, "Monthly spatial calibration of Blaney-Criddle equation for calculating monthly ET<sub>o</sub> in south of Iran," *Irrig. Drain.*, vol. 58, no. 2, pp. 234–245, 2009, doi: 10.1002/ird.409.
- [32] N. Seenu\*, D. R. M. K. Chetty, T. Srinivas, K. M. A. Krishna, and D. A. Selokar, "Reference Evapotranspiration Assessment Techniques for Estimating Crop Water Requirement," *Int. J. Recent Technol. Eng.*, vol. 8, no. 4, pp. 1094–1100, 2019, doi: 10.35940/ijrte.d6738.118419.
- [33] F. O. Akinyemi, M. Ikanyeng, and J. Muro, "Land cover change effects on land surface temperature trends in an African urbanizing dryland region," *City Environ. Interact.*, vol. 4, no. 2019, p. 100029, 2019, doi: 10.1016/j.cacint.2020.100029.